International Journal of Smart Sensor and Adhoc Network

Volume 1 | Issue 2 Article 21

2011

Sensorless Control of PMBLDC Motor Based on Speed Independent Position Function

C. Subba Rami Reddy
Electrical & Electronics Engineering Department , K.S.R.M College of Engineering, Kadapa, India,
c_subbramireddy2020@yahoo.com

M. Surya Kalavathi
Electrical & Electronics Engineering Department , J.N.T.U.H College of Engineering, Hyderabad, India,
munagala12@yahoo.co.in

Sensorless Control of PMBLDC Motor Based on Speed Independent Position Function

C. Subba Rami Reddy[1] & M. Surya Kalavathi[2]

[1]Electrical & Electronics Engineering Department , K.S.R.M College of Engineering, Kadapa, India
[2]Electrical & Electronics Engineering Department , J.N.T.U.H College of Engineering, Hyderabad, India
E-mail : c_subbramireddy2020@yahoo.com[1], munagala12@yahoo.co.in[2]

Abstract **-** This paper presents the methodology and implementation of a novel sensorless control technique for the permanent magnet brushless dc (PMBLDC) motor. In this new sensorless control technique, a novel flux linkage function is defined, which is speed independent. A physically insightful speed-independent function of flux linkage along with the combination of two differential equations governing the stator phase windings have been used for this purpose. The proposed new sensorless method solves the problem of sensorless PMBLDC motor at low speeds.

Keywords **-** *permanent magnet brushless dc motor; position function; speed control; sensorless.*

I. INTRODUCTION

A motion system based on the classic dc motor provides a good, simple and efficient solution to satisfy the requirements of a variable speed drive. Although dc motors possess good control characteristics and ruggedness, their performance and applications in wider areas is inhibited due to sparking and commutation problems [1]. Induction motor do not possess the above mentioned problems, they have their own limitations such as low power factor and non-linear speed torque characteristics [2]. With the advancement of technology and development of modern control techniques, the permanent magnet brushless dc (PMBLDC) motor is able to overcome the limitations mentioned above and satisfy the requirements of a variable speed drive [1,3].

The brushless dc (BLDC) motor is increasingly being used in computer, aerospace, military, automotive, industrial and household products because of its high torque, compactness, and high efficiency [4-7]. The PMBLDC motor is inherently electronically controlled and requires rotor position information for proper commutations of current. However, the problems of the cost and reliability of rotor position sensors have motivated research in the area of position sensorless BLDC motor drives [8,9]. This paper presents a novel sensorless position detection technique with a new physical concept based on a speed independent position function for the PMBLDC motors. With the speed independent position function, the commutation instants can be estimated from near zero (1.5% of the rated speed) to high speeds. Since the shape of the position function is identical at all speeds, it provides precise commutation pulse at steady state as well as transient state. The proposed method does not rely on the measured back electro motive force (EMF) and hence the need for external hardware circuitry for sensing terminal voltages is removed.

II. OVERVIEW OF SENSORLESS CONTROL TECHNIQUES

Sensorless methods for the trapezoidal back EMF type of PMBLDC motors [10,11] can be classified as follows.

- Back EMF sensing technique
- Back EMF integration technique
- Flux linkage based technique
- Freewheeling diode conduction

All these methods rely on speed dependent back EMF. Since the back EMF is zero or undetectably small at standstill and low speeds, it is not possible to use the back EMF sensing method in the low speed ranges. Also, the estimated commutation points that are shifted by 30° from zero crossing of back EMF have position error in transient state. The flux estimation method also has significant estimation error at low speed, in which the voltage equation is integrated in a relatively large period of time [8]. To overcome the above drawbacks, a

novel method, based on a new speed-independent function, is proposed, one that is based on a new physical insight.

III. PROPOSED SENSORLESS CONTROL TECHNIQUE

A. Principle

The general voltage equation of one of the active phases is given by

$$v_x = Ri_x + \sum_{k=1}^{n} \frac{d\psi_{kx}(\theta, i_x)}{dt} \quad (1)$$

Where v_x is the active phase voltage, R is the phase resistance, i_x is the phase current, θ is the rotor position, $\psi_{kx}(\theta, i_x)$ is the total flux linkage of the active phase and n is the number of phases. The flux linkage in the active phase includes both self and mutual flux linkages. For three-phase BLDC motors, the total flux linkage of the phase A is

$$\psi_A = L_{aa}(\theta,i_a).i_a + L_{ab}(\theta,i_b).i_b + L_{ac}(\theta,i_c).i_c + \lambda_{ar}(\theta) \quad (2)$$

Where, the first term, $L_{aa}(\theta, i_a).i_a$, represents the self flux linkage of phase A, the second and third term stand for the mutual flux linkage with phases B and C and the fourth term, $\lambda_{ar}(\theta)$ stands for the flux linkage due to the permanent magnet that is attached on the rotor. The first three terms of "(2)" are function of current and position, and the $\lambda_{ar}(\theta)$ is the function of position. Therefore, the flux profile has a close relationship with the dynamic performances. Since the BLDC motor uses permanent magnets, the permeability of the attached permanent magnet is considered as that of air, and hence, typically, the motor has small inductance variation. Therefore, if the motor is operated within the rated current, the saturation effect of inductance due to current level is usually neglected. For the surface-mounted permanent magnet (SMPM) type of BLDC motors, the permanent magnets are roundly attached on the round surface of the rotor, and hence, the inductance variation by rotor position is negligibly small. Based on the characteristics of the SMPM type of BLDC motors, the flux profile can be simplified as in "(3)" along with the following assumptions:

- The motor is operated within the rated condition and hence the saturation effect due to current level is neglected.
- The leakage inductance is negligibly small and hence neglected.
- Iron losses are negligible.

$$\psi_A = L_{aa} \cdot i_a + L_{ab} \cdot i_b + L_{ac} \cdot i_c + \lambda_{ar}(\theta) \quad (3)$$

Substituting "(3)" into "(1)" gives

$$v_a = R_a i_a + \frac{d}{dt}\left(L_{aa}i_a + L_{ab}i_b + L_{ac}i_c\right) + \frac{d\lambda_{ar}(\theta)}{dt} \quad (4)$$

In balanced three-phase BLDC motors

$$L_{aa} = L_{bb} = L_{cc} = L_s \quad (5)$$

$$L_{ba} = L_{ab} = L_{ca} = L_{ac} = L_{bc} = L_{cb} = M \quad (6)$$

where, L_s and M represent the self-inductance and mutual-inductance, respectively.

Substituting "(5)" and "(6)" into "(4)" gives

$$v_a = R_a i_a + \frac{d}{dt}\left(L_{aa}i_a + Mi_b + Mi_c\right) + \frac{d\lambda_{ar}(\theta)}{dt} \quad (7)$$

For a balanced star connected BLDC motors,

$$i_a + i_b + i_c = 0 \quad (8)$$

Using "(8)", "(7)" is simplified as

$$v_a = R_a i_a + L\frac{di_a}{dt} + \frac{d\lambda_{ar}(\theta)}{dt} \quad (9)$$

where $L = L_s - M$ is the phase inductance under balanced conditions.

The last term in the voltage equations is so called back EMF, and the term is redefined as

$$v_a = R_a i_a + L\frac{di_a}{dt} + \frac{d\left(k_e f_{ar}(\theta)\right)}{dt} \quad (10)$$

$$v_a = R_a i_a + L\frac{di_a}{dt} + k_e \cdot \frac{d\theta}{dt} \cdot \frac{d\left(f_{ar}(\theta)\right)}{d\theta} \quad (11)$$

where k_e stands for the back EMF constant.

It is seen that $\lambda_{ar}(\theta)$ in "(9)" is expressed as a constant value times a flux linkage function that is changed only by the rotor position as shown in "(10)". The $f_{ar}(\theta)$ is a flux linkage form function that is a function of rotor position. Since some manufacturers do not provide a motor neutral point, the line-to-line voltage equations are used as follows:

$$V_{ab} = R(i_a - i_b) + L\frac{d(i_a - i_b)}{dt} + k_e \cdot \omega \cdot \frac{d\{f_{ar}(\theta) - f_{br}(\theta)\}}{d\theta} \quad (12)$$

$$V_{ab} = R(i_a - i_b) + L\frac{d(i_a - i_b)}{dt} + k_e \cdot \omega \cdot \frac{df_{abr}(\theta)}{d\theta} \quad (13)$$

Where ω stands for the instantaneous speed. The $f_{abr}(\theta)$ is a line-to-line flux linkage form function that is a function of the rotor position. Now we define a new function, $H(\theta)_{ab}$, as

$$H(\theta)_{ab} = \frac{df_{abr}(\theta)}{d\theta} \quad (14)$$

Then, $H(\theta)_{ab}$ can be derived as

$$H(\theta)_{ab} = \frac{1}{\omega \cdot k_e}\left[(V_a - V_b) - R(i_a - i_b) - L\left(\frac{di_a}{dt} - \frac{di_b}{dt}\right)\right] \quad (15)$$

Since the $H(\theta)_{ab}$ function itself has a one to one relationship with rotor position, it is possible to use this function for position estimation. But as shown in "(15)", to know the $H(\theta)_{ab}$ function, the instantaneous speed term, that is unknown for dynamic operations, is required to calculate the function.

To eliminate the instantaneous speed term, ω, that causes trouble in using the $H(\theta)_{ab}$ function for position estimation, one line- to-line $H(\theta)$ function is divided by another line-to- line $H(\theta)$ function, and the divided new speed independent function is named $G(\theta)$. For example

$$G(\theta)_{bc/ab} = \frac{H(\theta)_{bc}}{H(\theta)_{ab}} = \frac{\left[(V_b - V_c) - R(i_b - i_c) - L\left(\frac{di_b}{dt} - \frac{di_c}{dt}\right)\right]}{\left[(V_a - V_b) - R(i_a - i_b) - L\left(\frac{di_a}{dt} - \frac{di_b}{dt}\right)\right]} \quad (16)$$

Fig.1 shows the $G(\theta)$ functions $G(\theta)_{bc/ab}$, $G(\theta)_{ab/ca}$ and $G(\theta)_{ca/bc}$, waveform based on "(15)". The standard commutation instant is when the $G(\theta)$ functions are changed from positive infinity to negative infinity as in Fig.1.

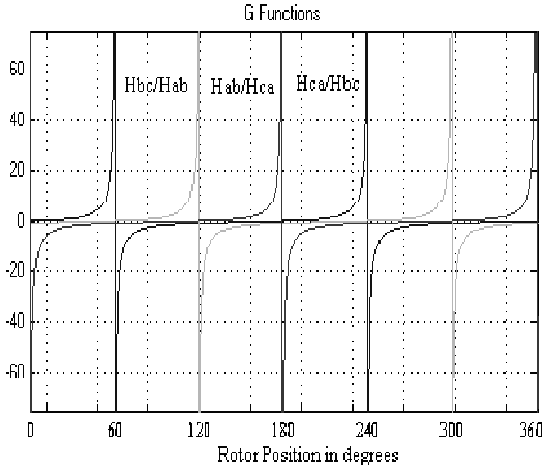

Fig. 1 : G Function waveforms

B. Commutation Strategy

After careful investigation of the shape of $G(\theta)$ function to provide the best indirect position-function that is speed-independent with high sensitivity at each commutation point, the ratio of two line-to-line $H(\theta)$ functions is sequentially utilized.

From the sequential combination of two line-to-line $H(\theta)$ functions at each commutation interval, the ideal $G(\theta)$ function that is independent of speed and contains continuous position information is derived. It means that only the positive part of the $G(\theta)$ function waveform in fig.1 is utilized. It is noted that the standard commutation point is the peak point of ideal $G(\theta)$ function that is the most sensitive part of the function as shown in fig.2. Therefore, the position estimation based on the $G(\theta)$ function can provide the best accuracy at commutation points of the current which are the most important instants for the sensorless operation.

Table I shows the position estimation equations at each mode in fig. 2. Two line-to-line $H(\theta)$ functions are used in each mode as Table I. As shown in fig. 2, at mode 1, $G(\theta)_1$ is used as a position estimation equation and after a 60° electrical angle, at mode 2, $G(\theta)_2$ is utilized. The time duration of each mode in fig.2 corresponds to 60° by electrical angles.

When the $G(\theta)$ function reaches a predefined threshold value, the motor is commutated. From the sequential combination of the $H(\theta)$ functions based on Table I, the $G(\theta)$ function can be made as shown in fig.2. It is noted that the commutation signal can be generated at the peak point that is the most sensitive part of the $G(\theta)$ function. From the available stator current and dc link voltage, the $G(\theta)$ function is computed based on the equations of Table I in real time. Since the waveform of the $G(\theta)$ function is identical at the entire speed range, it can be characterized at steady state in a look-up table, and used as a position reference for sensorless operation at all speeds.

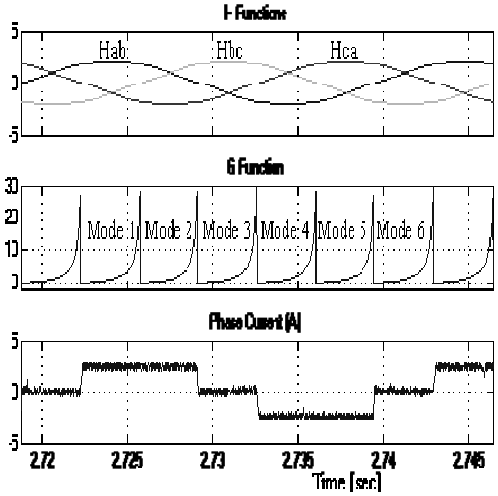

Fig. 2 : Line-to-line H Functions, G Function, Phase Current using proposed sensorless method

TABLE I : G FUNCTION AT EACH MODE

Mode	G Function
Mode 1 and 4	$G(\theta)_1 = \frac{H(\theta)_{ca}}{H(\theta)_{bc}} = \frac{V_{ca} - Ri_{ca} - L\frac{di_{ca}}{dt}}{V_{bc} - Ri_{bc} - L\frac{di_{bc}}{dt}}$
Mode 2 and 5	$G(\theta)_2 = \frac{H(\theta)_{bc}}{H(\theta)_{ab}} = \frac{V_{bc} - Ri_{bc} - L\frac{di_{bc}}{dt}}{V_{ab} - Ri_{ab} - L\frac{di_{ab}}{dt}}$
Mode 3 and 6	$G(\theta)_3 = \frac{H(\theta)_{ab}}{H(\theta)_{ca}} = \frac{V_{ab} - Ri_{ab} - L\frac{di_{ab}}{dt}}{V_{ca} - Ri_{ca} - L\frac{di_{ca}}{dt}}$

C. Current Control

To control currents, hysteresis controller can be used for the proposed sensorless method. Also, to calculate line-to-line voltages in equations in Table I at each mode, every phase current is actively controlled. It means that a silent phase current is controlled as zero

IV. SIMULATION RESULTS

The parameters of the PMBLDC motor used for simulation are as follows.

Power	: 1 HP
Rated speed	: 3500 rpm
Poles	: 4
Rated current	: 5 A
Rated torque	: 2 N-m
Inverter voltage	: 160 V
Armature resistance	: 0.75 Ω
Armature inductance	: 3.05 mH
Back EMF constant	: 0.21486 Vsec/rad
Torque constant	: 0.21476 Nm/A
Rotor inertia	: 8.2614e-4 Kg-m^2
Viscous friction coefficient	: 0.02 Nm/rad/ses.

Fig. 3 shows the block diagram of proposed sensorless control of PMBLDC motor. The complete drive system consists of a PMBLDC motor fed by a three-phase PWM inverter, speed independent position G function block and controller. The inverter which is connected to the dc supply feeds controlled power to the motor. The magnitude and frequency of the inverter output voltage depends on the switching signals generated by the hysteresis controller. The state of these switching signals at any instant is determined by mode of operation, speed error and winding currents. The controller synchronizes the winding currents with the mode given by G function. It also facilitates the variable speed operation of the drive and maintains the motor speed to reference value even during load variations [12-14].

The proposed sensorless control algorithm is verified through simulation using MATLAB SIMULINK package. Figs. 4 and 5 illustrate the performance of the proposed sensorless method at 1500 and 100 rpm.

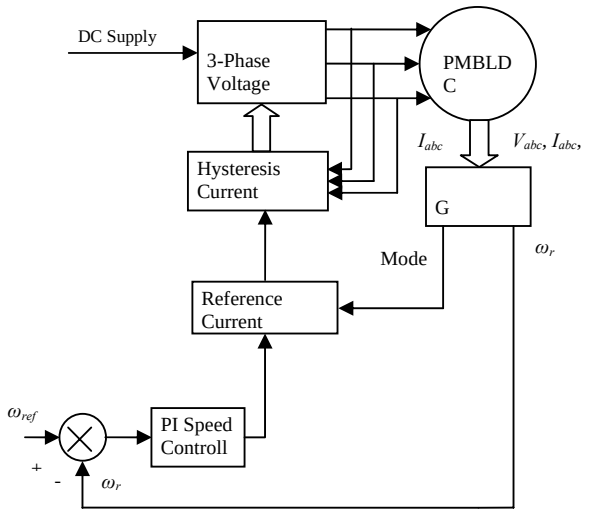

Fig. 3 : Block diagram of proposed sensorless control of PMBLDC drive.

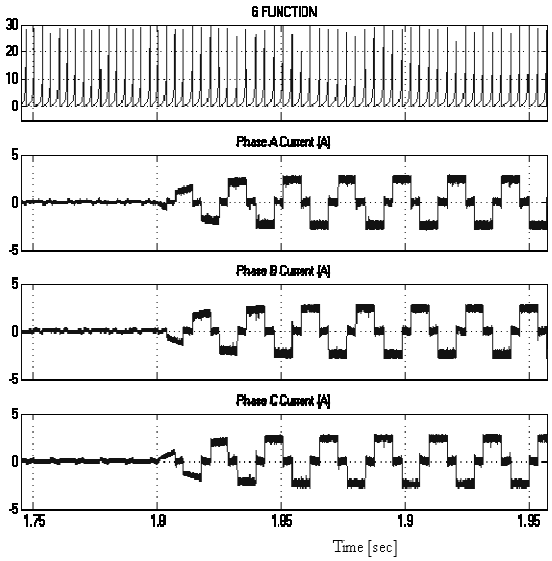

Fig. 4(a) : G Function and current waveforms for a step change in load of 1Nm at t=1.8sec (Reference speed = 1500 rpm).

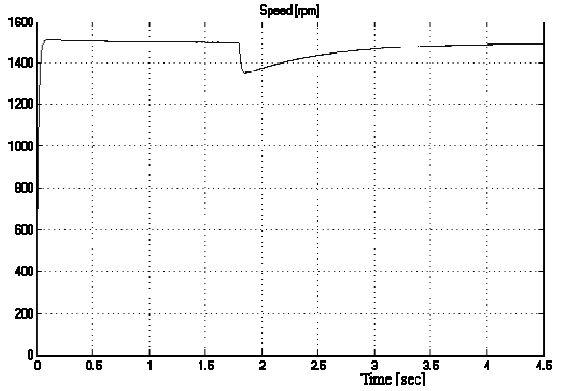

Fig. 4(b) : Variation of speed for a step change in load of 1Nm at t=1.8sec (Reference speed = 1500rpm).

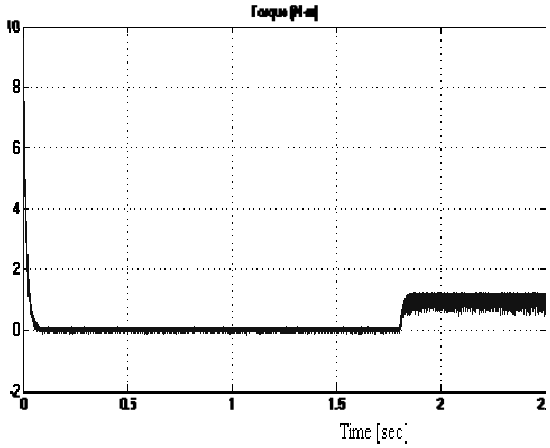

Fig. 4(c) : Electromagnetic torque variation for a step change in load of 1Nm at t=1.8sec (Reference speed = 1500 rpm).

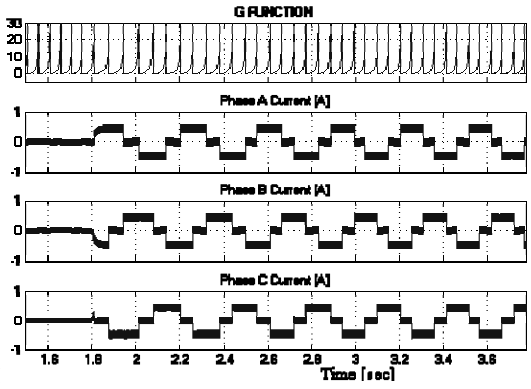

Fig. 5(a): G Function and current waveforms for a step change in load of 0.2Nm at t=1.8sec (Reference speed = 100 rpm).

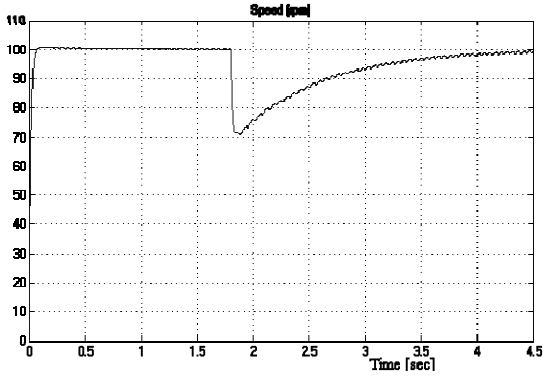

Fig. 5(b) : Variation of speed for a step change in load of 0.2 Nm at t=1.8sec (Reference speed = 100rpm)

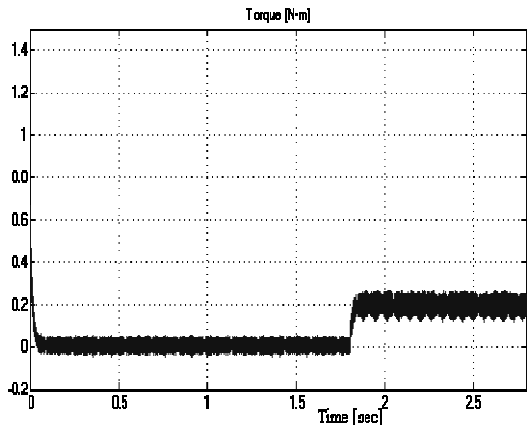

Fig. 5(c) : Electromagnetic torque variation for a step change in load of 0.2 Nm at t=1.8sec (Reference speed = 100rpm).

V. CONCLUSION

This paper presents a novel sensorless drive method for PMBLDC motors. This technique makes it possible to detect the rotor position over a wide speed range. This method provides commutation even in transient state because of the speed independent characteristics of $G(\theta)$ function.

REFERENCES

[1] W. Hong, W. Lee and B. K. Lee, "Dynamic simulation of brushless dc motor drives considering phase commutation for automotive applications", IEEE International Electric Machines & Drives Conference, 2007. IEMDC 2007. pp.1377-1383, 3-5 May 2007.

[2] T. J. E Miller, “Brushless permanent magnet and reluctance motor drives”, clarendon press, oxford, 1989.

[3] Paul C. Krause, “Analysis of Electric Machinery”, McGraw Hill Book Company, 1989.

[4] B K Bose, “Intelligent Control and Estimation in Power Electronics and Drives”, Electrical Machines and Drives Conference Record, IEEE international 18-21 may 1997,pp.TA2/2.1-TA2/2.6.

[5] H. Le-Huy, “Modeling and simulation of electrical drives using matlab/simulink and power system blockset”, The 27thannual conference of the IEEE Industrial Electronic Society (IECON’01), Denvor/Colorado, pp.1603-1611.

[6] Lee, P.W and Pollock, C, “Rotor Position Detection Techniques for Brushless Permanent-Magnet and Reluctance Motor Drives”, Industry Applications Society Annual Meeting, 1992, Conference Record of the 1992 IEEE, 4-9 Oct. 1992, pp.448-455 vol.1 Digital Object Identifier 10.1109/IAS.1992.244361.

[7] A. Kusko and S. M. Peeran, “Definition of the brushless DC motor,” Proc. of the IEEE Industry Application Society Annual Meeting IAS’88, pp. 20–22, 1988.

[8] N. Ertugrul and P. Acarney, “A new algorithm for sensorless operation of permanent magnet motors.” IEEE Trans. on Industry Applications, Vol. 30, pp. 126-133, Jan./Feb. 1994.

[9] Johnson J. P, Ehsani M and Guzelgunler Y, “Review of Sensorless Methods for Brushless DC,” in Proc. IEEE IAS’99 Conf., Vol. 1, 1999, pp. 143-150.

[10] T. Kim and M. Ehsani, “Advanced sensorless drive techniques for brushless dc motors,” U.S. Patent 60/438,949, 2004.

[11] M. Cirstea, A. Dinuaand and S. Redpath, “Modelling a New Sensorless Control Strategy for Brushless DC Motors,” IEEE International Conference on Industrial Technology (ICIT), 2004, pp. 408-413.

[12] B. K. Lee and M. Ehsani, “Advanced Simulation Model for Brushless DC Motor Drives,” Electric Power Components and Systems, Vol. 31, pp. 841-868, 2003.

[13] R. Wu and G. R. Selmon, “A permanent magnet motor drive without position sensor,” IEEE Trans. on Industry Applications, Vol. 27, pp. 1005-1011, Sept./Oct. 1991.

[14] P.Pillay and R.Krishnan, “Modeling simulation and Analysis of Permanent Magnet Motor Drives, Part-II: The Brushless DC Motor Drive,” IEEE Trans. on Industry Application, Vol. 25, No. 2, pp. 274-279, March/April1989.

◈◈◈